DSR Design for Scientific RENAISSANCE

JACSTR

Kinematics and Dynamics Representation Study of Upper-Limb Exoskeleton

Siti Khadijah Ali[1*] and M. Osman Tokhi
[1*] Faculty of Computer Science and Information Technology, Universiti Putra Malaysia, Serdang, Malaysia
[2] School of Engineering, London South Bank University, London, United Kingdom

Article Info

Received: 1 August 2018
Accepted: 1 September 2018
Published online: 1 December 2018

Abstract An exoskeleton has been identified as one of the solution to human muscle fatigue. The objective of this paper is to study the dynamics of the developed exoskeleton for designing the control system. The Denavit-Hartenberg (DH) and closed form solution are implemented to study the forward and inverse kinematics. The Euler-Lagrange approach is used to develop the dynamic system of the exoskeleton. The comparative study using Simmechanics in terms of the torque required is used to validate the dynamics representation. The results show that the torque generated from the Euler-Lagrange were similar in shape with the Simmechanics.

Keywords: **Kinematics and dynamics; Euler-Lagrange approach; Denavit-Hartenberg (DH); Muscle fatigue.**

1. Introduction

Muscle fatigue is a natural phenomenon that occurs due to inability of muscle to exert force in response to a voluntary effort. Muscle fatigue could occur to healthy people and patients, especially to those who are undergone rehabilitation such as post-stroke patients [1]. This problem not only could cause the reduction of power, but also lead to discomfort and pain. If the fatigue muscle is not treated or assisted, it could lead to musculoskeletal disorder (MSD) and cumulative trauma disorder (CDT) [2], [3], [4], [5], [6].

Fatigue is known to be dependent on the activation level, stimulation frequency and recovery and has an active relationship with muscle dynamics [1]. The endurance time and muscle contraction levels are the two parameters used to predict the occurrence of fatigue. Several techniques have been designed to directly assess the occurrence of fatigue. The example of a direct approach for estimating the fatigue is by observing or measuring the reduction of maximum voluntary contraction (MVC) or force output. The measurement is done after the activity. The indirect approaches are by examining or observing the endurance time, the EMG signals or muscle fibre twitch interpolation [7].

Several types of fatigue models are developed to avoid the associated health problems in the working population such as [8], [9], [10], [11] and [3]. In general, most of the developments of fatigue model, are used to identify the occurrence of fatigue and to reduce the MSDs by identifying suitable postures during work. These models are used in ergonomics research for industrial applications. Another technique to reduce the fatigue, is by supporting human with an exoskeleton. Several works have been done to investigate the capability of the exoskeletons in supporting and helping human in performing tasks.

An exoskeleton could be categorised based on the application, human-interaction mechanical design, control approach or techniques. In terms of application, exoskeleton has been developed to provide support to patients during rehabilitation [12], [13]. An exoskeleton has also been developed for assisting people with a limited range of arm movements during activities of daily living (ADL) [14], [15], [16]. Furthermore, an exoskeleton has been developed to augment healthy people while carrying physical tasks [17-18]. During the development of the exoskeleton, it is essential to ensure that the control strategy is effective, so that the exoskeleton could be operated harmoniously with the human upper-extremity. Therefore, in this work, the kinematics and dynamics of the developed exoskeleton are studied, as a preparation for designing the control strategy.

2. Methodology

A. System Description

SolidWorks are used to remodel the humanoid and to re-design the upper-extremity exoskeleton (Figure 1) because it allows to design complex 3D realistic models. In addition, the designs can easily be imported to other software/ applications such as VisualNastran and Simmechanics. The human is developed to presents the human-like physical system in terms of measurements of mass, height and length (Figure 1(a)). The measurements for the length and mass of human model are taken from [12] (Table I). The design of an exoskeleton used in this work is inspired by TitanArm [19]. This design is chosen because it is simple, capable of powered use and data transmission in a mobile fashion. The exoskeleton was designed with aluminium to provide the exoskeleton structure with a relatively light weight, since aluminium is a low-density material and has reasonable strength characteristics. The exoskeleton is designed to be worn on the lateral side of the upper limb to provide naturalistic movements of the shoulder, elbow and wrist joint (Figure 1). The designed exoskeleton has four revolute joints. The human-exoskeleton design, is then imported to Simmechanics for control system evaluation purpose.

Figure 1: The exoskeleton is attached parallel to human

B. Kinematics of the designed exoskeleton

Kinematics and dynamics are the two terms mostly used in robotic research. Kinematics is defined as the study of motion without considering the force, torque and moment. Two groups of kinematics are, forward kinematics and inverse kinematics. Forward kinematics is a process of obtaining the end-effector position when the angles of the joints are given. Inverse kinematics is a process of calculating the angles of the joints when the end-effector position is given..

Forward Kinematic: The Denavit-Hartenberg (DH) convention is used to obtain forward kinematics. The DH notation is chosen because it allows to compose coordinate transformation into one homogenous transformation matrix. The homogenous transformation matrix provides the relative position and orientation of two consecutive frames. This information is used to connect two consecutive frames. The two consecutive frames could be described as *i-1* and *i*. As shown in Figure 2 (a), the base frame for the exoskeleton is denoted as O_o. The O_o. also represents the shoulder adduction/abduction motion. The O_1, O_2 and O_3 represent shoulder internal/external motion, shoulder extension/flexion and elbow extension/flexion respectively. O4 represents the end-point of the exoskeleton.

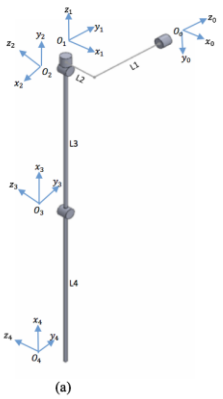

(a)

Frame	θ_i	α_i	d_i	a_i
1	θ_1	$\frac{\pi}{2}$	L_1	L_2
2	$\theta_2 - \frac{\pi}{2}$	$\frac{\pi}{2}$	0	0
3	$\theta_3 + \frac{\pi}{2}$	0	0	L_3
4	θ_4	0	0	L_4

(b)

Figure 2: (a) Schematic diagram (b) Denavit-Hartenberg table

In Figure 2 (b), the DH table consists of four parameters: θ_i, α_i, a_i,and d_i, where i = 0, 1, 2, …. n.

1) θ_i, represents the angle between X_{i-1} and X_i measured around Z_{i-1}

2) α_i represents the angle between X_{i-1} and Z_i measured around X_i
3) a_i is the distance along X_i from O_i to the intersection of the axis X_i and Z_{i-1}
4) d_i is the distance along Z_{i-1} from O_{i-1} to the intersection of X_i and Z_{i-1} axes

There are steps to determine the frame for each joint. The first step is to determine the origin of the axes, denoted by O_i. The z-axis designates the direction of motion for each joint. The O_1, O_2, O_3 and the z-axes for the designed exoskeleton are shown as in Figure 3. The following step is to determine the x-axes for the joints. There are three rules to choose the direction of the x-axis. The rules are based on the position of the Z_{i-1} and Z_i, and are given as follows:

1) If the Z_{i-1} and Z_i are not co-planar, there exists a unique line segment perpendicular to both Z_{i-1} and Z_i. This line defines x-axis for frame i.
2) If the Z_{i-1} and Z_i are parallel, there exists an infinite line segments perpendicular to Z_{i-1} and Zi, and the X-axis for frame i can be chosen from one of these lines. There are two options for choosing the direction of the X-axis; could be pointing to Z_{i-1} and not pointing to Z_{i-1}. For this category, the $d_i$and a_i, both will be equal to 0.
3) If the Z_{i-1} and Z_i are intersecting, the X_i is chosen normal to the plane formed by Z_{i-1} and Z_i. For this case, the ai would be equal to 0. The final step is the assignment of the Y-axes. The Y-axis is gathered using the right-hand rule.

The homogenous transformation can be obtained by:

$$T_i^{i-1} = Rot(Z,\theta_1)Trans(Z,d_i)Trans(X,a_i)Rot(X,\alpha_i) \qquad (1)$$

Using equation (1), the individual homogenous transfer matrix that relate two successive frames can be obtained. After substituting the DH parameter into equation (1), the homogenous transformation matrix for frame 1, frame 2, frame 3 and frame 4 can be obtained as:

$$T_1^0 = \begin{pmatrix} c(\theta_1) & 0 & s(\theta_1) & L_2 * c(\theta_1) \\ s(\theta_1) & 0 & -c(\theta_1) & L_2 * s(\theta_1) \\ 0 & 1 & 0 & L_1 \\ 0 & 0 & 0 & 1 \end{pmatrix} \qquad (2)$$

$$T_2^1 = \begin{pmatrix} s(\theta_2) & 0 & -c(\theta_2) & 0 \\ -c(\theta_2) & 0 & -c(\theta_2) & 0 \\ 0 & 1 & 0 & 0 \\ 0 & 0 & 0 & 1 \end{pmatrix} \qquad (3)$$

$$T_3^2 = \begin{pmatrix} -s(\theta_3) & -c(\theta_3) & 0 & -L_3 * s(\theta_3) \\ c(\theta_3) & -s(\theta_3) & 0 & L_3 * c(\theta_3) \\ 0 & 0 & 1 & 0 \\ 0 & 0 & 0 & 1 \end{pmatrix} \qquad (4)$$

$$T_4^3 = \begin{pmatrix} c(\theta_4) & -s(\theta_4) & 0 & L_4 * c(\theta_4) \\ s(\theta_4) & c(\theta_4) & 0 & L_4 * s(\theta_4) \\ 0 & 0 & 1 & 0 \\ 0 & 0 & 0 & 1 \end{pmatrix} \qquad (5)$$

The homogenous transformation matrix that relates frame 4 to frame 0 can be obtained as:

$$T_4^0 = [T_1^0 . T_2^1 . T_3^2 . T_4^3] \quad (6)$$

This represents the position and orientation of the end-effector (frame 4 / axis-4) with respect to the fixed reference frame (frame 0 / axis-0). The homogenous transformation matrix in equation (6) can be presented in a simplified form as:

$$T_4^0 = \begin{bmatrix} R_4^0 & P_4^0 \\ 0 & 1 \end{bmatrix} \quad (7)$$

where R_4^0 represents the orientation and P_4^0 the position of the end-effector. The position information that is gathered from the homogenous transformation matrix in equation (7) will be used in inverse kinematics to derive the dynamics of the designed exoskeleton.

Inverse Kinematic: The inverse kinematics may be obtained with two ways: closed form and numerical solution. Numerical method is used if the closed form solution fails or is too difficult to obtain. Closed-form solution, on the other hand, could give indefinite solutions. Hence, a specification is needed to ensure the right solution. Since the structure of the exoskeleton is not complex, closed form solution is considered. Specifically, the algebraic method of closed form solution is used to obtain the inverse kinematics in this work. As shown in Figure 3, the exoskeleton has four joints and are described with θ_1, θ_2, θ_3, and θ_4. Theθ_1, θ_2, θ_3, and $\theta_4$represent the angle of shoulder abduction/adduction, shoulder internal/external, shoulder extension/flexion and elbow extension/flexion respectively. In this work, θ_2, makes no different in terms of the position of the end-effector as shown in Table II. Therefore, in this work, there is no need to obtain the inverse kinematic for θ_2. θ_2 is also restricted to rotate between -60 to 60.

Table II: The end-effector positions with different values of θ_2

θ_2 (rad)	x_4	y_4	z_4
0	0.1777	-0.7023	0.1354
0.1754	0.1777	-0.7023	0.1354
-0.1754	0.1777	-0.7023	0.1354

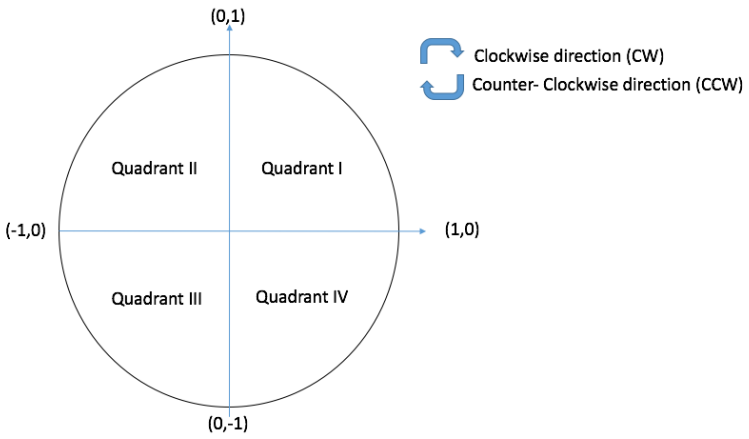

Figure 3: Unit circle

As mentioned earlier, closed-form approach could give more than one solution. There is a possibility for one angle to obtain two signs (+ and -). Hence, by using unit circle as shown in Figure 3, a unique solution could be obtained. The unit circle consists of length with radius 1.

For θ_1, the range is in quadrant I and II of unit circle. The θ_1, is obtained by

$$\theta_1 = tan^{-1}\left(\frac{y_1}{x_1}\right) \tag{8}$$

The x_1 and y_1 are gathered from equation (2).

For θ_3 (equation (9)), the range is in quadrant I and II of unit circle and the sign is determined by the axis of x_1. It is known that in the Cartesian coordinate, the axes of x and y are divided into positive (x >0 and y>0) and negative (x ≤0 and y≤0). The x_3 and y_3 could be obtained from equation (4) as follows:

$$\theta_3 = cotan^{-1}\left(\frac{y_3}{-x_3}\right) \tag{9}$$

The algorithm to obtain θ_3 is shown as

Algorithm 1 Algorithm for θ_3

1: If $x_3 \leq 0$ && $\frac{-pi}{2} \leq \theta_3 \leq 0$
2: $\theta_{3final} = pi + \theta_3$
3: elseif $x_3 \leq 0$ && $0 \leq \theta_3 \leq \frac{pi}{2}$
4: $\theta_{3final} = \theta_3$
5: elseif $x_3 \geq 0$ && $\frac{-pi}{2} \leq \theta_3 \leq 0$
6: $\theta_{3final} = \theta_3$
7: elseif $x_3 \geq 0$ && $0 \leq \theta_3 \leq \frac{pi}{2}$
8: $\theta_{3final} = -(pi - \theta_3)$

The θ_4 is obtained by

$$\theta_4 = tan^{-1}\left(\frac{y_4}{x_4}\right) \tag{10}$$

Similar as θ_3, the sign for θ_4 is determined by the position of the axis x4. The algorithm for obtaining the $\theta_4$is shown as follows:

Algorithm 2 Algorithm for θ_4

1: If $x_4 \geq 0$
2: $\theta_{4final} = \theta_4$
3: elseif $x_4 \leq 0$ && $\frac{-pi}{2} \leq \theta_4 \leq 0$
4: $\theta_{4final} = pi + \theta_4$
5: elseif $x_4 \leq 0$ && $0 \leq \theta_4 \leq \frac{pi}{2}$
6: $\theta_{4final} = -(pi - \theta_4)$

C. Dynamics of the exoskeleton

The dynamics of the system are defined as the study of the motion considering the moment, force or torque. In this work, the dynamic system of the designed exoskeleton is developed by Euler-Lagrange approach because it is frequently used for modelling multi-rigid robotic systems. It contains the kinetic energy and potential energy. The Lagrangian can be described as L = T - V where, T is the kinetic energy and V is the potential energy of the system. The Lagrangian is a function of generalized coordinates, q_j and generalized velocities, $\dot{q}_j$, which be represented as:

$$L = L\left(q_1, q_2, q_3, \ldots\ldots, q_j, \dot{q}_1, \ldots\ldots\ \dot{q}_j, \ldots, \dot{q}_d\right) \tag{11}$$

where the d is the number of degree of freedom.

In this research, the d is four. Thus, the equation (11) become L = L (q_1, q_2, q_3, q_4, $\dot{q}_1$, $\dot{q}_2$, $\dot{q}_3$, $\dot{q}_4$). The kinetic energy, T and the potential energy, V, for the designed exoskeleton are obtained by differentiating the vector position for each joint. The position vectors for the joints (θ_1, θ_2, θ_3, θ_4) with respect to the fixed coordinate system are presented as:

$$\begin{pmatrix} x_1 \\ y_1 \\ z_1 \end{pmatrix} = \begin{pmatrix} L_2\cos(\theta_1) \\ L_2\sin(\theta_1) \\ L_1 \end{pmatrix} \tag{12}$$

$$\begin{pmatrix} x_2 \\ y_2 \\ z_2 \end{pmatrix} = \begin{pmatrix} L_2\cos(\theta_1) \\ L_2\sin(\theta_1) \\ L_1 \end{pmatrix} \tag{13}$$

$$\begin{pmatrix} x_3 \\ y_3 \\ z_3 \end{pmatrix} = \begin{pmatrix} L_2c_1 + L_3s_1c_3 - L_3c_1s_3s_2 \\ L_2s_1 - L_3c_1c_3 - L_3s_1s_2s_3 \\ L_1 + L_3s_3c_2 \end{pmatrix} \tag{14}$$

$$\begin{pmatrix} x_4 \\ y_4 \\ z_4 \end{pmatrix} = \begin{pmatrix} L_2c_1 + L_4c_4 * (s_1c_3 - c_1s_3s_2) + \\ L_4s_4(-s_3s_1 - c_1c_3s_2) + L_3s_1c_3 - \\ L_3c_1s_3s_2L_2s_1 - L_4c_4(c_1c_3 + s_3s_1s_2) - \\ L_4s_4(-c_1s_3 + s_1c_3s_2) - L_3c_1c_3 - L_3s_3s_1s_2 \\ L_1 + L_3s_3c_2 + L_4c_4s_3c_2 + L_4s_4c_3c_2 \end{pmatrix} \tag{15}$$

Where c_1, c_2, c_3, c_4, s_1, s_2, s_3, s_4 are cos(θ_1), cos(θ_2), cos(θ_3), cos(θ_4), sin(θ_1), sin(θ_2), sin(θ_3)
and sin(θ_4).

The (x_i, y_i), in equations (12-15) are differentiated and shown below:

$$\begin{pmatrix} \dot{x}_1 \\ \dot{y}_1 \end{pmatrix} = \begin{pmatrix} -L_2\sin(\theta_1)\dot{\theta}_1 \\ L_2\cos(\theta_1)\dot{\theta}_1 \end{pmatrix} \tag{16}$$

$$\begin{pmatrix} \dot{x}_2 \\ \dot{y}_2 \end{pmatrix} = \begin{pmatrix} -L_2 \sin(\theta_1)\dot{\theta}_1 \\ L_2 \cos(\theta_1)\dot{\theta}_1 \end{pmatrix} \tag{17}$$

$$\begin{pmatrix} \dot{x}_3 \\ \\ \dot{y}_3 \end{pmatrix} = \begin{pmatrix} L_3c_1c_3\dot{\theta}_1 - L_2s_1\dot{\theta}_1 - L_3s_1s_3\dot{\theta}_3 - L_3c_1c_2s_3\dot{\theta}_2 - \\ L_3c_1c_3s_2\dot{\theta}_3 + L_3s_1s_2s_3\dot{\theta}_1 \\ L_2c_1\dot{\theta}_1 + L_3c_3s_1\dot{\theta}_1 + L_3c_1s_3\dot{\theta}_3 - L_3c_1s_2s_3\dot{\theta}_1 - \\ L_3c_2s_1s_3\dot{\theta}_2 - L_3c_3s_1s_2\dot{\theta}_3 \end{pmatrix} \tag{18}$$

$$\begin{pmatrix} \dot{x}_4 \\ \dot{y}_4 \end{pmatrix} = \begin{pmatrix} L_3c_1c_3\dot{\theta}_1 - L_2s_1\dot{\theta}_1 - L_3s_1s_3\dot{\theta}_3 + \\ L_4c_1c_3c_4\dot{\theta}_1 - L_3c_1c_2s_3\dot{\theta}_2 - \\ L_3c_1c_3s_2\dot{\theta}_3 - L_4c_1s_3s_4\dot{\theta}_1 - \\ L_4c_3s_1s_4\dot{\theta}_3 - L_4c_4s_1s_3\dot{\theta}_3 - \\ L_4c_3s_1s_4\dot{\theta}_4 - L_4c_4s_1s_3\dot{\theta}_4 + \\ L_3s_1s_2s_3\dot{\theta}_1 - L_4c_1c_2c_3s_4\dot{\theta}_2 - \\ L_4c_1c_2c_4s_3\dot{\theta}_2 - L_4c_1c_3c_4s_2\dot{\theta}_3 - \\ L_4c_1c_3c_4s_2\dot{\theta}_4 + L_4c_3s_1s_2s_4\dot{\theta}_1 + \\ L_4c_4s_1s_2s_3\dot{\theta}_1 + L_4c_1s_2s_3s_4\dot{\theta}_3 + \\ L_4c_1s_2s_3s_4\dot{\theta}_4 \\ L_2c_1\dot{\theta}_1 + L_3c_3s_1\dot{\theta}_1 + L_3c_1s_3\dot{\theta}_3 + \\ L_4c_3c_4s_1\dot{\theta}_1 + L_4c_1c_3s_4\dot{\theta}_3 + \\ L_4c_1c_4s_3\dot{\theta}_3 + L_4c_1c_3s_4\dot{\theta}_4 + \\ L_4c_1c_4s_3\dot{\theta}_4 - L_3c_1s_2s_3\dot{\theta}_1 - \\ L_3c_2s_1s_3\dot{\theta}_2 - L_3c_3s_1s_2\dot{\theta}_3 - \\ L_4s_1s_3s_4\dot{\theta}_1 - L_4c_1c_3s_2s_4\dot{\theta}_1 - \\ L_4c_1c_4s_2s_3\dot{\theta}_1 - L_4c_2c_3s_1s_4\dot{\theta}_2 - \\ L_4c_2c_4s_1s_3\dot{\theta}_2 - L_4c_3c_4s_1s_2\dot{\theta}_3 - \\ L_4c_3c_4s_1s_2\dot{\theta}_4 + L_4s_1s_2s_3s_4\dot{\theta}_3 + \\ L_4s_1s_2s_3s_4\dot{\theta}_4 \end{pmatrix} \tag{19}$$

The total kinetic energy, T of the whole system is given by:

$$\begin{aligned} T(q,\dot{q}) = \frac{1}{2}(m_1(\dot{x}_1^2 + \dot{y}_1^2) + m_2(\dot{x}_2^2 + \dot{y}_2^2) + m_3(\dot{x}_3^2 + \dot{y}_3^2) + \\ m_4(\dot{x}_4^2 + \dot{y}_4^2)) + \\ \frac{1}{2}(I_1\dot{\theta}_1^2 + I_2(\dot{\theta}_1 + \dot{\theta}_2)^2 + I_3(\dot{\theta}_1 + \dot{\theta}_2 + \dot{\theta}_3)^2 + \\ I_4(\dot{\theta}_1 + \dot{\theta}_2 + \dot{\theta}_3 + \dot{\theta}_4)^2) \end{aligned} \tag{20}$$

The total potential energy of the four degree-of-freedom exoskeleton is presented as:

$$V(q) = m_1gy_1 + m_2gy_2 + m_3gy_3 + m_4gy_4 \tag{21}$$

Thus, equations (20) and (21) give the Lagrangians as:

$$L = T(q,\dot{q}) - V(q) \tag{22}$$

The dynamic equation can be obtained by applying partial derivatives to equation (22).

$$\frac{d}{dt}\left(\frac{\partial L}{\partial \dot{q}}\right) - \frac{\partial L}{\partial q} = \Gamma \tag{23}$$

A dynamic model of the exoskeleton (equation (23)) can be rewritten as:

$$M(q)\ddot{q} + C(q,\dot{q})\dot{q} + G(q) = \Gamma \tag{24}$$

In which $M(q)$ is the exoskeleton inertia matrix, $C(q,\dot{q})$ is a matrix containing the Coriolis and Centrifugal terms, $G(q)$ is a vector containing the gravity torques, τ is avector of external torques acting on the actuated degree-of-freedom (DOF) and $q, \dot{q}$ and $\ddot{q}$ are position, angular velocity and angular acceleration of the revolute joints.

The dynamic equation (equation (24)) was validated using Simmechanics (Figure 4). The validation process was done by applying angular position onto shoulder and elbow joints.

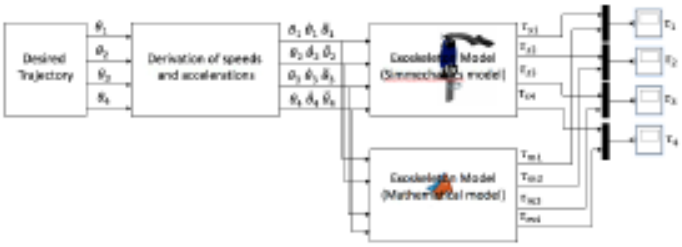

Figure 4: Simmechanics and Simulink diagram to simulate the dynamical system

3. Results and Discussion As mentioned earlier, the angular position is applied to the shoulder and elbow joints. Two different motions stated used (Figure 5): static and flexion-extension for shoulder and elbow joints.

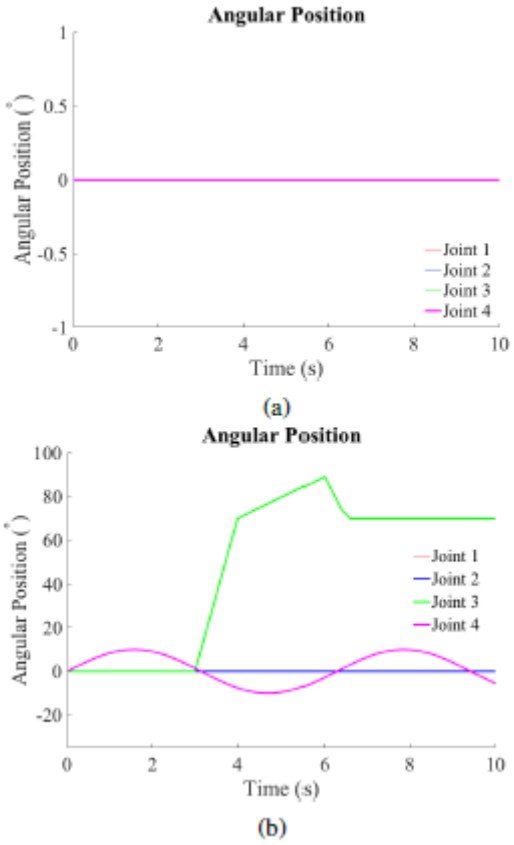

Figure 5: Angular position: (a) Static (b) Flexion-extension

Figure 6 and 7 show the angular velocity and torque measured from the static movement. It is obvious that these two measurements are 0 because there were no excitation applied to these joints.

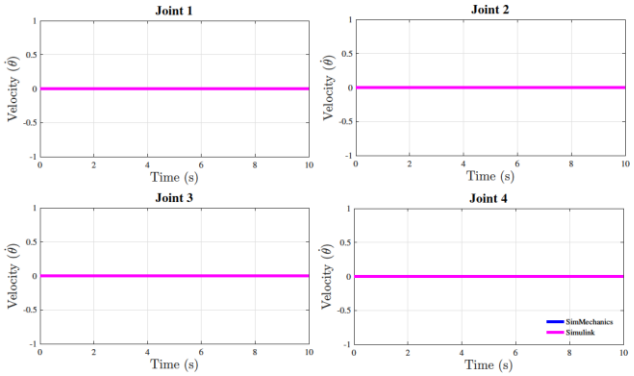

Figure 6: Angular velocity for static

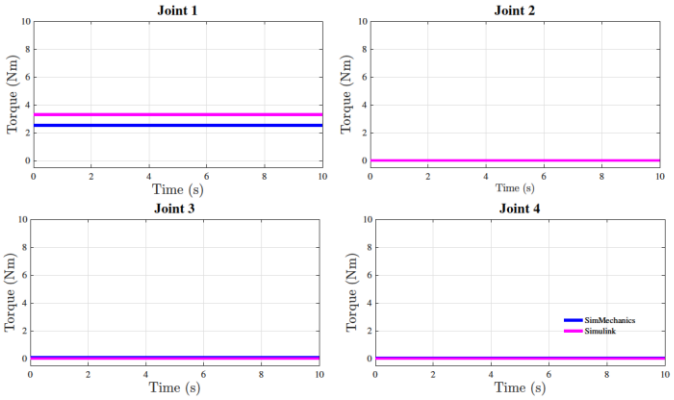

Figure 7: Torque for static

Meanwhile, Figure 8 and 9, show changes for both joints. Although, excitation was applied for flexion to shoulder joint and flexion-extension to elbow joint, the movement affected the torques of shoulder internal-external and shoulder abduction-adduction (Figure 10). This is due to the coupling effect of the exoskeleton. However, the effects were small.

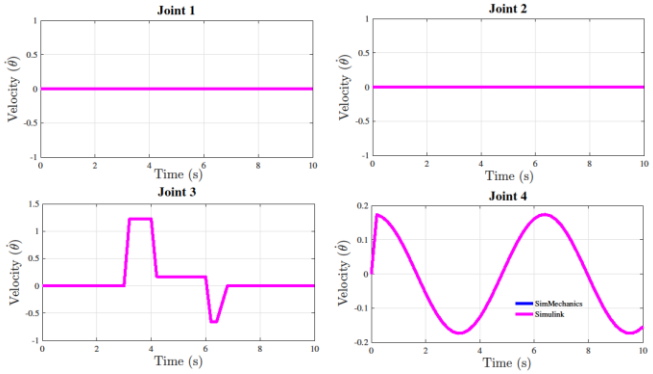

Figure 8: Angular velocity for flexion-extension

The pattern of the τ_1, τ_3 and τ_4 of the Simmechanics and the mathematical representation of the dynamic system of the exoskeleton were similar in shape, although were different in values (Figure 10). The torque generated from the mathematical representation (Simulink) was slightly higher than that from Simmechanics. This could be due to differences in the geometrical model built in Simmechanics and parameter described in the mathematical equation. However, for Joint_2, the pattern was different between Simmechanics and Simulink. However, the discrepancies are less than 0.5, and this can be considered insignificant.

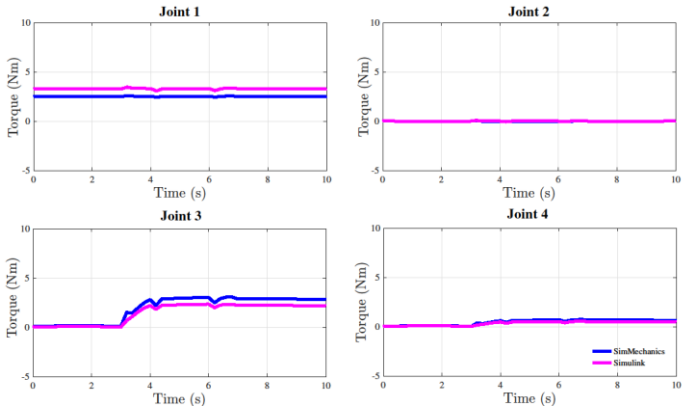

Figure 9: Torque for flexion-extension

4. Conclusions A study of the kinematics and dynamic representation for the upper-limb exoskeleton is presented in this work. A comparative study using Simmechanics is used to validate the dynamic (mathematical) representation. The results show that the torques generated by the mathematical representation were similar in shape with the Simmechanics. Hence, this could be concluded that, the dynamics representation is validated. Future work will focus on the development of the control system and an assessment of muscle fatigue.

5. Acknowledgement of this research was supported financially by the Ministry of Higher Education Malaysia (MOHE), Universiti Putra Malaysia and University of Sheffield.

References

1. Xu, W., Chu, B., & Rogers, E. (2014). Iterative learning control for robotic-assisted upper limb stroke rehabilitation in the presence of muscle fatigue. *Control Engineering Practice*, *31*, 63-72.
2. Seth, D., Chablat, D., Bennis, F., Sakka, S., Jubeau, M., & Nordez, A. (2016). Validation of a new dynamic muscle fatigue model and dmet analysis. *The International Journal of Virtual Reality*, *2016*(16).
3. Sakka, S., Chablat, D., Ma, R., & Bennis, F. (2015). Predictive model of the human muscle fatigue: application to repetitive push-pull tasks with light external load. *arXiv preprint arXiv:1503.06391*.
4. Ma, R., Chablat, D., & Bennis, F. (2013). A new approach to muscle fatigue evaluation for Push/Pull task. In *Romansy 19–Robot Design, Dynamics and Control* (pp. 309-316). Springer, Vienna.
5. Ma, L., Chablat, D., Bennis, F., & Zhang, W. (2009). A new simple dynamic muscle fatigue model and its validation. *International Journal of Industrial Ergonomics*, *39*(1), 211-220.
6. Ma, L., Bennis, F., Chablat, D., & Zhang, W. (2008, April). Framework for dynamic evaluation of muscle fatigue in manual handling work. In *Industrial Technology, 2008. ICIT 2008. IEEE International Conference on* (pp. 1-6). IEEE.

7. Zhang, Z., Li, K. W., Zhang, W., Ma, L., & Chen, Z. (2014). Muscular fatigue and maximum endurance time assessment for male and female industrial workers. *International Journal of Industrial Ergonomics*, *44*(2), 292-297.
8. Liu, J. Z., Brown, R. W., & Yue, G. H. (2002). A dynamical model of muscle activation, fatigue, and recovery. *Biophysical journal*, *82*(5), 2344-2359.
9. Ma, L., Chablat, D., Bennis, F., Zhang, W., Hu, B., & Guillaume, F. (2011). A novel approach for determining fatigue resistances of different muscle groups in static cases. *International Journal of Industrial Ergonomics*, *41*(1), 10-18.
10. Ma, L., Chablat, D., Bennis, F., Zhang, W., & Guillaume, F. (2010). A new muscle fatigue and recovery model and its ergonomics application in human simulation. *Virtual and Physical Prototyping*, *5*(3), 123-137.
11. Ma, R., Chablat, D., Bennis, F., & Ma, L. (2012). Human muscle fatigue model in dynamic motions. In *Latest Advances in Robot Kinematics* (pp. 349-356). Springer, Dordrecht.
12. Głowiński, S., Krzyżyński, T., Pecolt, S., & Maciejewski, I. (2015). Design of motion trajectory of an arm exoskeleton. *Archive of Applied Mechanics*, *85*(1), 75-87.
13. Ochoa Luna, C., Habibur Rahman, M., Saad, M., Archambault, P. S., & Bruce Ferrer, S. (2015). Admittance-based upper limb robotic active and active-assistive movements. *International Journal of Advanced Robotic Systems*, *12*(9), 117
14. Chen, C. J., Cheng, M. Y., & Su, K. H. (2013, November). Observer-based impedance control and passive velocity control of power assisting devices for exercise and rehabilitation. In *Industrial Electronics Society, IECON 2013-39th Annual Conference of the IEEE* (pp. 6502-6507). IEEE.
15. Kiguchi, K. (2007). Active exoskeletons for upper-limb motion assist. *International Journal of Humanoid Robotics*, *4*(03), 607-624.
16. Kiguchi, K., & Hayashi, Y. (2012). An EMG-based control for an upper-limb power-assist exoskeleton robot. *IEEE Transactions on Systems, Man, and Cybernetics, Part B (Cybernetics)*, *42*(4), 1064-1071.
17. de Looze, M. P., Bosch, T., Krause, F., Stadler, K. S., & O'Sullivan, L. W. (2016). Exoskeletons for industrial application and their potential effects on physical work load. *Ergonomics*, *59*(5), 671-681.
18. Rashedi, E., Kim, S., Nussbaum, M. A., & Agnew, M. J. (2014). Ergonomic evaluation of a wearable assistive device for overhead work. *Ergonomics*, *57*(12), 1864-1874
19. Beattie, E., McGill, N., Parrotta, N., & Vladimirov, N. (2012). Titan: A Powered, Upper-Body Exoskeleton. *Retrieved November*, *22*, 2014.